ELSEVIER

Materials Science and Engineering A 471 (2007) 63–68

MATERIALS SCIENCE & ENGINEERING A

www.elsevier.com/locate/msea

Microstructural evolution and mechanical properties of friction stir welded Mg–Zn–Y–Zr alloy

G.M. Xie [a,b], Z.Y. Ma [a,*], L. Geng [b], R.S. Chen [a]

[a] *Institute of Metal Research, Chinese Academy of Sciences, Shenyang 110016, China*
[b] *School of Materials Science and Engineering, Harbin Institute of Technology, Harbin 150001, China*

Received 7 January 2007; received in revised form 27 February 2007; accepted 13 March 2007

Abstract

Six millimetre thick Mg–Zn–Y–Zr plate was friction stir welded (FSW). Under a tool rotation rate of 800 rpm and a traverse speed of 100 mm/min, the defect-free weld was obtained. After FSW, coarse strip-like microstructure in forged Mg–Zn–Y–Zr alloy changed into fine equiaxed recrystallized grains in the nugget zone. Furthermore, bulky I-phase particles were broken up and dispersed with some of them being transformed to W-phase, and most of MgZn precipitates were dissolved. Micro-hardness measurement indicated that the hardness of the nugget zone was higher than that of the parent material and the lowest value of hardness was found in the heat-affected zone (HAZ). Transverse tensile tests showed that the strengths and elongation of the weld was only slightly lower than those of parent material with ultimate tensile strength of the weld reaching 95% of the parent material.

Keywords: Friction stir welding; Magnesium alloy; Microstructure; Mechanical property

1. Introduction

Requirement for increasing fuel efficiency and transportation speed of space probes and cars promoted high-speed development of even light alloys, thus magnesium alloy with high specific strength has been successfully applied to the structure parts [1]. However, the close-packed hexagonal structure of magnesium alloy resulted in limited strength and ductility at room temperature. To improve mechanical properties of magnesium alloy, extensive researches have been focused on alloying and plastic processing.

Addition of Y element can provide the strengthening effect to magnesium alloys by the Orowan mechanism, especially at elevated temperatures [2]. Forged Mg–Zn–Y–Zr alloys have been produced by thermomechanical processes. In Mg–Zn–Y alloys, it was suggested that there were three kinds of ternary equilibrium phases, i.e. I-phase (Mg_3Zn_6Y), W-phase ($Mg_3Zn_3Y_2$) and Z-phase ($Mg_{12}ZnY$) [3–5]. However, the Z-phase was identified only in the Mg–1.2Zn–7.2Y–0.48Zr alloy with high Y content and low Zn/Y ratio [6]. For Mg–Zn–Y–Zr alloys, zirconium does not take part in the formation of secondary phases [7]. Therefore, in the forged Mg–Zn–Y–Zr alloys with low yttrium content, the main phases were I-phase and W-phase [8–13], and some Mg–Zn aging strengthening phases were also detected [9].

With fast development and wide applications, the welding of magnesium alloys becomes a main concern. The drawbacks associated with the fusion welding include: (a) complex thermal stresses and severe deformation, (b) the presence of porosity and crack in the fusion zone, (c) the excess eutectic formation. Friction stir welding (FSW) is a relatively new solid-state joining technique, invented by The Welding Institute of the UK in 1991 [14]. A non-consumable rotating tool with a specially designed pin and shoulder is inserted into the abutting edges of sheets or plates to be joined and traversed along the line of joint to form the weld. Since the invention of FSW, most efforts focused on high-strength aluminum alloys [15]. The close-packed hexagonal structure of magnesium alloy results in the lack of slip plane during plastic processing, therefore, it is more difficult to obtain sound FSW joint of magnesium alloys than that of the aluminum alloys.

In the past few years, a number of studies have been conducted to evaluate the feasibility of FSW of magnesium alloys. From the investigations on AZ (Mg–Al–Zn) and AM

* Corresponding author. Tel.: +86 24 83978908; fax: +86 24 83978908.
E-mail address: zyma@imr.ac.cn (Z.Y. Ma).

0921-5093/$ – see front matter © 2007 Elsevier B.V. All rights reserved.
doi:10.1016/j.msea.2007.03.041

(Mg–Al–Mn) series magnesium alloys it was seen that sound FSW joints with good properties and uniform microstructure can be achieved under optimized FSW parameters [16–25]. While Nakata et al. [22] and Lee et al. [23] reported that sound joints were produced only at higher tool rotation rates and lower traverse speeds in thixomolded AZ91D and hot-rolled AZ31B-H24, the investigations by Lee et al. [24] and Park et al. [25] indicated that defect-free FSW welds of AZ91D could be achieved at relatively high tool rotation rates of 800–1600 rpm for a wide range of tool traverse speeds. To the best of our knowledge, no attempt has been made so far to evaluate the weldability of Mg–Zn–Y–Zr alloy via FSW. In this study, we reported the first result on FSW of Mg–Zn–Y–Zr alloy.

2. Experimental procedure

Mg–Zn–Y–Zr alloy forging with a composition of 6.0Zn–0.6Y–0.6Zr (in wt.%) was used for this study. The plates of 6 mm in thickness, 300 mm in length and 70 mm in width were machined from the forging and welded at a tool rotation rate of 800 rpm and a traverse speed of 100 mm/min by using a gantry FSW machine (China FSW Center). A tool with a shoulder of 22 mm in diameter and a coniform threaded pin of 6 mm in diameter and 5.7 mm in length was used. The tilt angle for all welds was maintained at 2.5°. Before welding, the plates were cleared by the wire brush to remove surface oxide layer. The FSW samples were cross-sectioned perpendicular to the welding direction, polished and then etched with solution of 90 ml ethanol, 10 ml distilled water, 5 ml acetic acid and 5 g picric acid. Microstructural features were characterized by optical microscopy (OM) and scanning electron microscopy (SEM). Grain sizes were measured by the mean linear intercept method. Distribution of element and composition of phase in the nugget zone and the parent material (PM) were analyzed by the Oxford type energy dispersive spectroscopy (EDS) and Philips type X-ray diffractometer (XRD), respectively. The Vickers-hardness of the joint was measured with a 500 g load for 13 s by LECO-LM247AT type Vickers-hardness machine. The tensile specimens with a gauge length of 40 mm and a gauge width of 10 mm were machined perpendicular to the FSW direction. The tensile test was carried out using the Zwick-Roell type testing machine at a strain rate of $4.2 \times 10^{-4}\ s^{-1}$.

3. Results and discussion

Fig. 1 shows the typical cross-sectional macrographs of FSW Mg–Zn–Y–Zr joint. No welding defect was detected in the joint, indicating that the sound FSW Mg–Zn–Y–Zr joint can be achieved under investigated welding parameter (rotation rate of 800 rpm and traverse speed of 100 mm/min). As in FSW aluminum alloys, three microstructural zones were identified, i.e. nugget zone, thermomechanically affected zone (TMAZ) and heat-affected zone (HAZ). The nugget zone exhibited a basin-like shape, which is similar to that observed in FSW AZ31 [26]. Fig. 2 shows the microstructures of the parent material, TMAZ and nugget zone. The parent material exhibited a typical as-forged structure, characterized by coarse strip-like structures and large secondary phase particles with the fine dynamic recrystallized grains being distributed between coarse strip-like structures (Fig. 2(a)). In the TMAZ, the dynamic recrystallization did not occur due to insufficient deformation strain and thermal exposure, and the elongated grains with coarse secondary phase particles being distributed along flow line were observed (Fig. 2(b)). Intense plastic deformation and frictional heating during FSW resulted in the generation of fine recrystallized grains of 6.8 μm within the nugget zone (Fig. 2(c)). The grain size of the nugget zone was significantly smaller than that of the parent material. Similarly, Esparza et al. [18] and Park et al. [27] reported the generation of the recrystallized grains of 10–15 μm in the nugget zone of FSW AZ61 and AM60 alloys [17,27]. Beyond the TMAZ there is a HAZ, which experienced a thermal cycle without any plastic deformation. The grain size in HAZ was coarser than that in the nugget zone with the precipitates being coarsened and/or dissolved into the matrix. Therefore, the HAZ was usually the weakest zone of FSW joint.

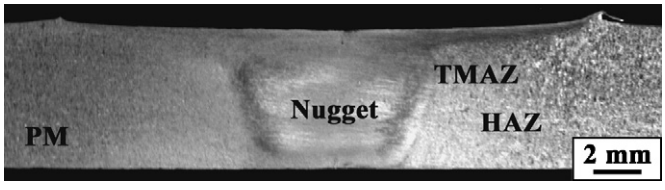

Fig. 1. Cross-sectional macrograph of FSW Mg–Zn–Y–Zr joint (the advancing side is on the right).

Fig. 3 shows the X-ray diffraction patterns of the parent material and nugget zone. For both parent material and nugget zone, the diffraction peaks of α-Mg, I-phase, W-phase, MgZn and $MgZn_2$ were detected. No Z-phase was detected due to lower Y content and higher Zn/Y ratio [6]. In a previous study [8], Zhang et al. reported the existence of α-Mg and I-phase in Mg–5.5Zn–0.7Y–0.4Zr (in wt.%) alloy with some weak diffraction peaks not being identified. This study indicated that these weak diffraction peaks correspond to MgZn and $MgZn_2$ phases. Fig. 4 shows SEM images of various microstructural zones. The secondary phase particles were quite coarse and the distribution was very heterogeneous in the parent material (Fig. 4(a)). In the TMAZ, the coarse secondary phase particles tended to be distributed along the flow lines and the size of the particles did not change (Fig. 4(b)). In the nugget zone, significantly refined secondary phase particles were homogeneously distributed in the magnesium matrix (Fig. 4(c)). This is attributed to significant breaking and dispersion effect of the threaded pin during FSW. The EDS analyses indicated that the secondary phase particles in both parent material and nugget zone correspond to the Mg–Zn–Y ternary phase (Fig. 5).

In solidification process of Mg–Zn–Y–Zr alloy, the eutectic temperatures of I-phase and W-phase were ~450 and 510 °C, respectively [8]. In this case, the solidification sequence of Mg–Zn–Y–Zr alloy was in turn W-phase, I-phase, and then Mg–Zn phase was formed. The formation of the I-phase and W-phase consumed most of the Zn element in the alloy, therefore ternary eutectic phases (I-phase and W-phase) in cast Mg–Zn–Y–Zr alloy were the main secondary phases. Because

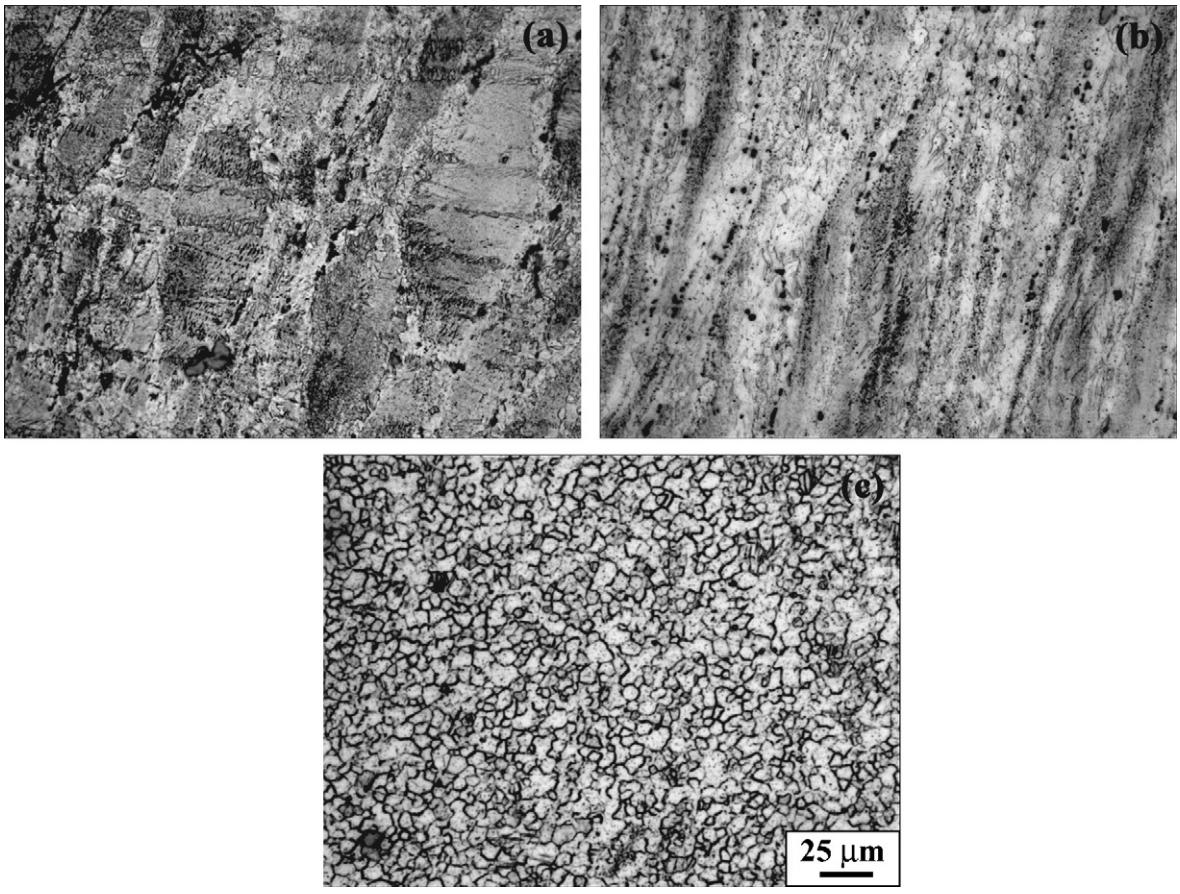

Fig. 2. Microstructure of Mg–Zn–Y–Zr alloy: (a) PM, (b) TMAZ, and (c) nugget zone.

the forging was conducted at a lower temperature of 390 °C, the eutectic phases (I-phase and W-phase) did not change after the forging. Fig. 6 showed the DSC results of the parent material and nugget zone. The two endothermic peaks appeared at ~340 and 458 °C in the parent material. Based on Ref. [8] and the present XRD analysis, the endothermic peak at 458 °C corresponds to the dissolution of I-phase. Besides, the precipitation temperature of the MgZn phase was about 340 °C [28], thus another endothermic peak was due to the dissolution of the MgZn phase. The W-phase and $MgZn_2$ phases, detected by the XRD pattern, were not observed in the DSC curve (Fig. 6), probably due to lower contents.

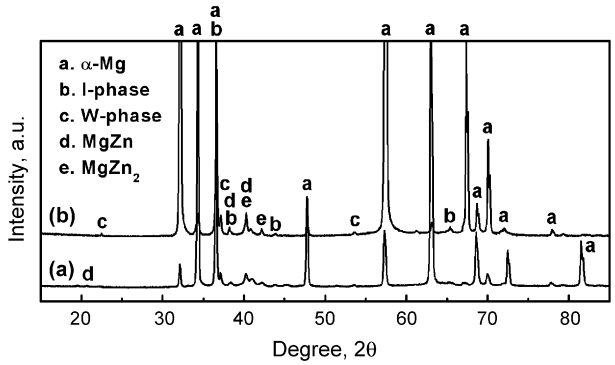

Fig. 3. XRD patterns of Mg–Zn–Y–Zr alloy: (a) PM and (b) nugget zone.

Recently, Zhang et al. studied the effect of Y content on the formation of the ternary eutectic phases in Mg–5.4Zn–(0.7–1.7)Y–0.4Zr (in wt.%) alloys [8]. With the Y content of ≤1.35 wt.%, the alloy consisted of α-Mg and I-phase, whereas for a higher Y content of 1.7 wt.%, the W-phase appeared. On the other hand, Lee et al. reported that the Zn/Y ratio exerted a significant effect on the types of ternary eutectic phases in as-cast Mg–Zn–Y alloys [29]. The phases identified in the as-cast microstructure were α-Mg + Mg_7Zn_3 with the Zn/Y ratio (wt.) of ~10, α-Mg + I-phase with the Zn/Y ratio of 5–7 (Y content: 0.5–1.6 wt.%), α-Mg + I-phase + W-phase with the Zn/Y ratio of 2–2.5 (Y content: 1.2–2.5 wt.%), and α-Mg + W-phase with the Zn/Y ratio of 1.5–2.0. For the Mg–6.0Zn–0.6Y–0.6Zr alloy in this study, the Zn/Y ratio is as high as 10 with a lower Y content of 0.6 wt.%. However, no Mg_7Zn_3 phase was identified, which is different from the observation in Ref. [29]. Further, in addition to the I-phase as the main phase in this forged Mg–Zn–Y–Zr alloy (Figs. 3(a) and 6), a small amount of the W-phase was also detected as shown by XRD pattern (Fig. 3(a)). This observation is not consistent with that in Ref. [8]. Clearly, the formation of the ternary eutectic phases in the Mg–Zn–Y–Zr alloys is quite complicated and dependent on both Y content and Zn/Y ratio [6,8,29]. More work is needed to elucidate the influencing factors.

For the nugget zone, two endothermic peaks were observed at ~460 and 500 °C and the endothermic peak corresponding

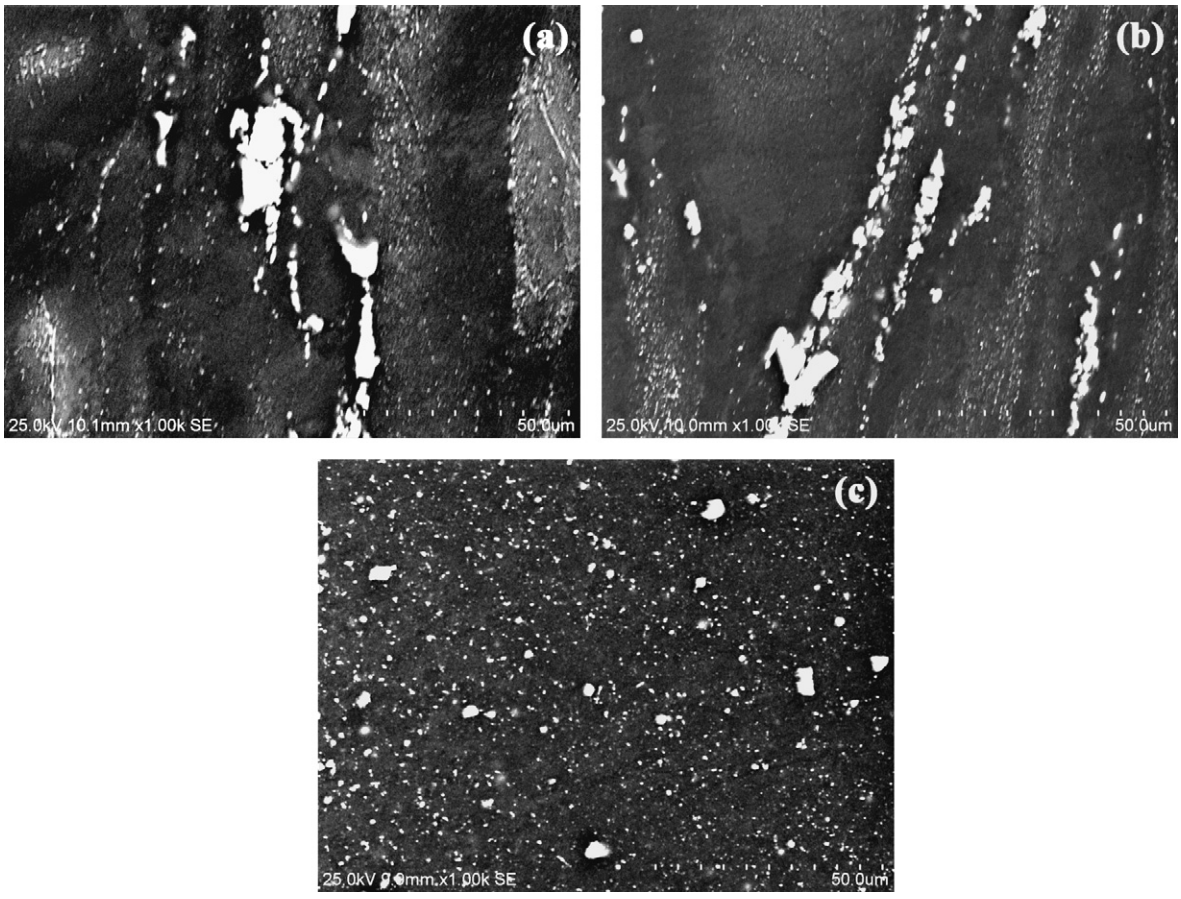

Fig. 4. SEM images of Mg–Zn–Y–Zr alloy: (a) PM, (b) TMAZ, and (c) nugget zone.

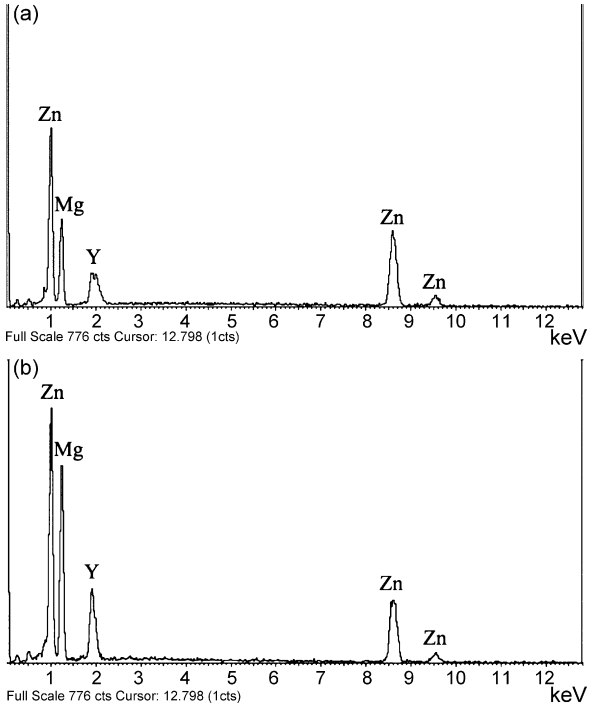

Fig. 5. EDS analysis of Mg–Zn–Y–Zr alloy: (a) PM and (b) nugget zone.

to the dissolution of the MgZn phase disappeared (Fig. 6). This indicates that most of the MgZn phase was dissolved into the magnesium matrix during the FSW cycle. Compared to the parent material, the intensity of the endothermic peak at ~460 °C in the nugget zone, corresponding to the dissolution of the I-phase, was significantly reduced, indicating that the amount of the I-phase was considerably decreased. On the other hand, the appearance of the endothermic peak at ~500 °C corresponding to the eutectic temperature of the W-phase indicated significant increase of the W-phase in the nugget zone. This implies that part of the I-phase was transformed to the W-phase during the

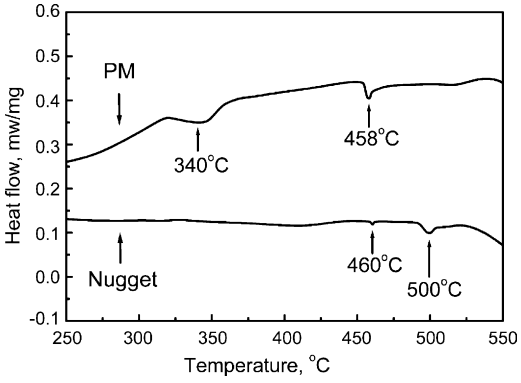

Fig. 6. Differential scanning calorimetry (DSC) curves of Mg–Zn–Y–Zr alloy.

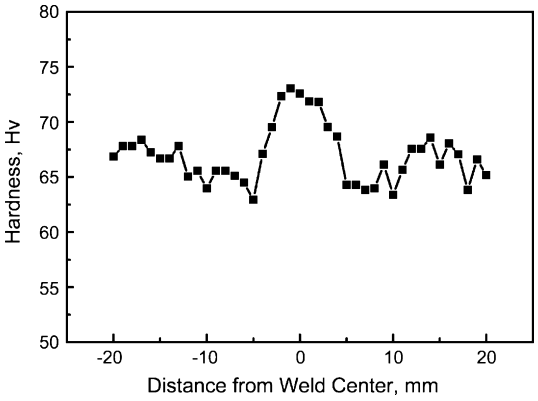

Fig. 7. Hardness profile of FSW Mg–Zn–Y–Zr joint.

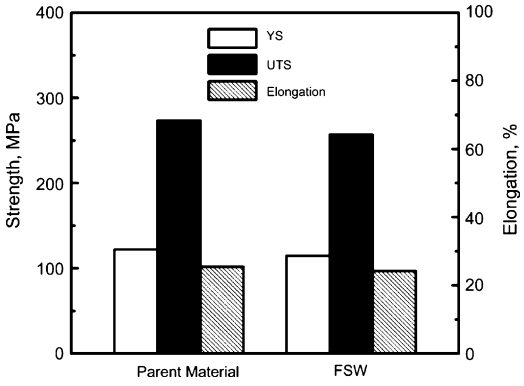

Fig. 8. Transverse tensile properties of PM and FSW joint.

FSW process. The exact mechanism for the transformation of the I-phase to the W-phase is not clear. One possible mechanism is that under high temperature and severe plastic deformation of the FSW, part of the I-phase was dissolved into the α-Mg and released Zn and Y promoted the growth of the W-phase or formed new W-phase in the region with a higher concentration of Y (lower Zn/Y ratio).

Based on the DSC curves and microstructural examinations, it is concluded that FSW resulted in significant grain refinement and breakup of the bulky I-phase and their dispersive distribution, at the same time, part of the I-phase was transformed to the W-phase and most of the MgZn phase was dissolved into the magnesium matrix. In a previous study, it was reported that friction stir processing (FSP) resulted in the generation of the fine recrystallized grains and significant breakup and dissolution of the coarse network-like eutectic β-$Mg_{17}Al_{12}$ phase in AZ91D casting [30]. The present result is consistent with that obtained in Ref. [30].

Fig. 7 shows the hardness profile along the centerline on the cross-section of the weld. The hardness values within the nugget zone were higher than that of the parent material. This is attributed to the generation of the fine recrystallized grains and dispersed ternary eutectic phases (I-phase and W-phase) in the nugget zone (Figs. 2(c) and 4(c)). Similarly, in FSP heat-proof Mg–Al–Ca alloy, it was reported that hardness values in the nugget zone were higher than that in the parent material due to the refined grains and porphyrization of bulky secondary phase [31]. Furthermore, the lowest hardness values were observed in the HAZ. This is attributed to the coarsening and/or dissolution of the MgZn precipitates during FSW thermal cycle. However, the decrease in the hardness of the HAZ over that of the parent material for this Mg–Zn–Y–Zr alloy is not so large as that for heat-treatable aluminum alloys [15,32] because soluble MnZn phase is not the main secondary phase in the alloy.

The transverse tensile properties for the FSW joint are shown in Fig. 8. Compared to the parent material, the FSW joint exhibited somewhat decreased ultimate tensile and yield strengths and elongation-to-failure. The fracture occurred in the HAZ on the retreating side, which is consistent with the lowest hardness distribution in the HAZ. In this case, the transverse tensile and yield strengths of the weld are those of the HAZ, i.e. the weakest zone in the whole weld. Therefore, although the nugget zone exhibited the highest hardness in the weld, slightly reduced tensile and yield strengths were observed when the weld was tested along the transverse direction. A similar observation has been made in FSW heat-treatable aluminum alloys [15,32]. Furthermore, the gage length (40 mm) of the tensile specimen cover the nugget zone, TMAZ, HAZ, and parent material zone, therefore, the observed elongation was contributed by all four zones. However, due to quite non-uniform hardness distribution over the whole gage length (Fig. 7), the deformation occurred mainly in the HAZ as well as the parent material zone, there was only limited deformation in the nugget zone due to higher hardness, therefore, reduced elongation was observed for the transverse tension of the weld compared to the parent material. In a previous study on FSW 7075Al-T651, Mahoney et al. [33] evaluated the deformation heterogeneity over various microstructural zones in transverse tensile specimens quantitatively. It was indicated that the deformation occurred mainly in the HAZ due to significantly reduced hardness.

Recently, Esparza et al. [18] and Gharacheh et al. [26] reported that the ultimate tensile strength of FSW AZ31 and AM60 joints was 81 and 93% of the parent materials, respectively. In this study, the ultimate tensile strength of the Mg–Zn–Y–Zr weld reached 95% of the parent material. The joining efficiency (UTS_{FSW}/UTS_{PM}) achieved for Mg–Zn–Y–Zr exceeded that for AZ31 and AM60 alloys. This indicates that FSW is a very effective technique for welding Mg–Zn–Y–Zr alloy.

4. Conclusions

(1) Under a rotation rate of 800 rpm and a traverse speed of 100 mm/min, 6 mm thick forged Mg–Zn–Y–Zr alloy plate was successfully friction stir welded and defect-free weld with basin-like nugget zone was obtained.
(2) During FSW, fine and equiaxed recrystallized grains of 6.8 μm were generated, bulky I-phases were broken up and dispersed with some of them being transformed to W-phase and most of MgZn phase was dissolved into the magnesium matrix.
(3) The strengths and elongation of the FSW joint was only slightly lower than those of the parent material. The joining efficiency was as high as 95%.

Acknowledgements

This work was supported by the National Outstanding Young Scientist Foundation for Z.Y. Ma under Grant No. 50525103, the National Basic Research Program of China under Grant No. 2006CB605205, and the Hundred Talents Program of Chinese Academy of Sciences.

References

[1] Z.H. Chen, Magnesium Alloy, China Chemical Industry Press, 2004, p. 446 (in Chinese).
[2] T. Mohiri, M. Mabuchi, N. Saitao, M. Nakamura, Mater. Sci. Eng. A 257 (1998) 287.
[3] E.M. Padezhnova, E.V. Mel'nik, R.A. Miliyevskiy, T.V. Dobatkina, V.V. Kinzhibao, Russ. Metall. (Metally) 4 (1982) 185.
[4] Z.P. Luo, S.Q. Zhang, J. Mater. Sci. Lett. 12 (1993) 1490.
[5] C. Janot, Quasicrystals, Clarendon Press, Oxford, 1994.
[6] Z.P. Luo, S.Q. Zhang, J. Mater. Sci. 19 (2000) 813.
[7] W.F. Smith (Ed.), Structure and Properties of Engineering Alloys, McGraw-Hill, New York, 1993, p. 542.
[8] Y. Zhang, X.Q. Zeng, L.F. Liu, C. Lu, H.T. Zhou, Q. Li, Y.P. Zhu, Mater. Sci. Eng. A 373 (2004) 320.
[9] D.K. Xu, L. Liu, Y.B. Xu, E.H. Han, Mater. Sci. Eng. A 420 (2006) 322.
[10] L.Y. Wei, L. Dunlop, H. Westengen, Metall. Mater. Trans. A 26 (1994) 1705.
[11] Z.P. Luo, D.Y. Song, S.Q. Zhang, J. Alloys Compd. 230 (1995) 109.
[12] D.H. Bae, S.H. Kim, D.H. Kim, W.T. Kim, Acta Mater. 50 (2002) 2343.
[13] L.Y. Wei, L. Dunlop, H. Westengen, Metall. Mater. Trans. A 26 (1994) 1947.
[14] W.M. Thomas, E.D. Nicholas, J.C. Needham, M.G. Murch, P. Templesmith, C.J. Dawes, G. B. Patent Application No. 9,125,978.8, December (1991).
[15] R.S. Mishra, Z.Y. Ma, Mater. Sci. Eng. R 50 (2005) 1.
[16] H. Zhang, S.B. Lin, L. Wu, J.C. Feng, S.L. Ma, Mater. Des. 27 (2006) 805.
[17] J.A. Esparza, W.C. Davis, E.A. Trillo, L.E. Murr, J. Mater. Sci. Lett. 21 (2002) 917.
[18] J.A. Esparza, W.C. Davis, L.E. Murr, J. Mater. Sci. 38 (2003) 941.
[19] S.H.C. Park, Y.S. Sato, H. Kokawa, Metall. Mater. Trans. A34 (2003) 987.
[20] X.H. Wang, K.S. Wang, Mater. Sci. Eng. A 431 (2006) 114.
[21] S. Lim, S. Kim, C.G. Lee, C.D. Yim, S.J. Kim, Metall. Mater. Trans. A36 (2005) 1609.
[22] K. Nakata, S. Inoki, Y. Nagano, T. Hashimoto, S. Johgan, M. Ushio, Proceedings of the Third International Symposium on Friction Stir Welding, Kobe, Japan, September 27–28, 2001.
[23] W.B. Lee, J.W. Kim, Y.M. Yeon, S.B. Jung, Mater. Trans. 44 (2003) 917.
[24] W.B. Lee, Y.M. Yeon, S.B. Jung, Mater. Sci. Technol. 19 (2003) 785.
[25] S.H.C. Park, Y.S. Sato, H. Kokawa, J. Mater. Sci. 38 (2003) 4379.
[26] M.A. Gharacheh, A.H. Kokabi, G.H. Daneshi, B. Shalchi, R. Sarrafi, Int. J. Mach. Tool Manuf. 46 (2006) 1983.
[27] S.H.C. Park, Y.S. Sato, H. Kokawa, Scr. Mater. 49 (2003) 161.
[28] S. Bhan, S. Lal, J. Phase Equilib. 14 (1993) 634.
[29] J.Y. Lee, D.H. Kim, H.K. Lim, D.H. Kim, Mater. Lett. 59 (2005) 3801.
[30] A.H. Feng, Z.Y. Ma, Scr. Mater. 56 (2007) 397.
[31] D.T. Zhang, S. Mayumi, M. Kouichi, Scr. Mater. 52 (2005) 899.
[32] Y.S. Sato, H. Kokawa, M. Enmoto, S. Jogan, Metall. Mater. Trans. 30A (1999) 2429.
[33] M.W. Mahoney, C.G. Rhodes, J.G. Flintoff, R.A. Spurling, W.H. Bingel, Metall. Mater. Trans. 29A (1998) 1955.